ASSESSMENT OF THE BOUSSINESQ APPROXIMATION FOR BUOYANCY-DRIVEN FLOWS

I. Di Piazza*and M. Mulas†
Area of Computational Fluid Dynamics, CRS4 - C.P. 94 , Uta(Ca) 09100, Italy
http://www.crs4.it/Areas/cfd/

ABSTRACT

The numerical simulation of buoyant flows often makes use of the Boussinesq approximation. This is particularly true when Direct Numerical Simulation is used for the analysis of heat transfer loops or other applications of natural convection flows. Boussinesq approximation consists of considering the density strictly constant, adding the buoyant force to the momentum balance and coupling an equation for the temperature to the incompressible Navier-Stokes system that has to be solved. In this paper, the validity of the Boussinesq approximation is investigated in some details via numerical simulations. The test cases chosen include a differentially heated cavity and two buoyant heated loops with internal heating. Results show clearly that the error on some performance parameters depends linearly on the compressibility parameter $\beta\Delta T$. The error in some cases can be 20% or higher, but it is drastically reduced to a few percent by the use of a 2^{nd} order formulation of the Boussinesq source term. Nevertheless, some flow features are strictly tied to the compressible coupling and are not captured in a Boussinesq framework.

1 INTRODUCTION

Although natural convection had not much been considered in the past for engineering applications, it has become increasingly important during the last decades. Nowadays, there are many practical flows configurations based on natural convection mechanism. A first example is the passive cooling systems in recent advanced nuclear reactor. Other examples are fire within buildings, solar collectors, and electronic components in enclosures. The numerical simulation of buoyant flows often makes use of the Boussinesq approximation. This is particularly true when Direct Numerical Simulation is used for the analysis of heat transfer loops or other applications of natural convection flows. Boussinesq approximation consists of considering the density strictly constant, adding the buoyant force to the momentum balance and coupling an equation for the temperature to the incompressible Navier-Stokes system that has to be solved.

What is missing in such a picture is the effect of compressibility which influences the velocity field through the continuity equation. Actually, the reversible energy exchange mechanism between internal and kinetic energy (the pdv work of thermodynamics) represents the true origin of motion in natural convection flows.

Application of Buckingham therorem to natural convection flows identifies three independent non dimensional parameters: the two well known Grashof and Prandlt numbers and a third parameter, independent of the other two, which can be for instance $\beta\Delta T$ and can be read as a measure of the compressibility of the system. The macroscopic thermo-fluid dynamic performance of a heat exchange buoyant loop is then given for instance by the Nusselt number dependence $Nu = Nu(Gr, Pr, \beta\Delta T)$.

The Boussinesq approximation is equivalent to add a source term in the momentum equation, neglecting the coupling between density and velocity field. The limiting value of $\beta\Delta T$ which would allow to neglect this effect is somehow arbitrary, and it is often imposed by the impossibility to do otherwise, rather than based upon the level of accuracy sought. The effects of compressibility in such flows is emerging as a hot problem and numerous works can be found in the most recent literature [1].

On the other hand most of the experimental works are confined to small temperature drops and therefore are not able to show up the problem.

Chenoweth and Paolucci [2] studied a differentially heated square cavity with large temperature difference for air. They observed a marginal influence of the compressibility parameter on the average wall heat flux, but a strong influence on the physical nature of the flow instabilities in the transition regime. More recently, Paillere *et al.* [1] investigated different numerical methods to solve low Mach number compressible flows in the same case as [2].

Possible examples of non-Boussinesq buoyant flows can be found in the context of natural convection buoyant loops in advanced nuclear power plants, where large temperature drops are needed in order to ensure fully turbulent motion and high heat transfer rates. Of course, other high-tech applications can show compressible buoyant effects.

The aim of this work is to assess the limits of the Boussinesq approximation by the use of numerical simulations. Computations are performed using a fully compressible coupled RANS Navier-Stokes solver capable of efficiently addressing flows in the whole regime of Reynolds, Mach and Grashof numbers. Thermodynamics is described in terms of general equation of

*e-mail: ivandp@crs4.it
†e-mail: mulas@crs4.it

state, this allows to take all terms into account and also to recover the Boussinesq formulation as a special case. A precise and quantitative evaluation of the effects of the approximation can be then obtained.

2 PROBLEM FORMULATION

2.1 Governing equations

The so-called fully compressible Navier-Stokes system of equations is considered:

$$\frac{\partial \rho}{\partial t} + \frac{\partial}{\partial x_j}(\rho u_j) = 0 \tag{1}$$

$$\frac{\partial \rho u_i}{\partial t} + \frac{\partial}{\partial x_j}(\rho u_i u_j + \delta_{ij} p - \tau_{ij}) = \rho g_i \tag{2}$$

$$\frac{\partial \rho E}{\partial t} + \frac{\partial}{\partial x_j}(\rho H u_j - u_i \tau_{ij} + q_j) = \dot{Q} \tag{3}$$

where H is the total enthalpy per unt volume and it is represented by $H \equiv E + p/\rho$. The total energy per unit mass E includes the internal and the kinetic energy as well as the gravitational potential $\Phi = gz$. τ_{ij} is the traceless viscous stress tensor defined as $\tau_{ij} = 2\mu S_{ij} - \frac{2}{3}\mu\delta_{ij}\frac{\partial u_i}{\partial x_i}$, and S_{ij} is the strain rate tensor $S_{ij} = \frac{1}{2}\left(\frac{\partial u_i}{\partial x_j} + \frac{\partial u_j}{\partial x_i}\right)$. A total stress tensor can be also defined as $\sigma_{ij} = -p\delta_{ij} + \tau_{ij}$ where pressure term is the reversible portion (tied to compressibility) while viscous stress tensor is the irreversible part. The system is fully coupled by a general equation of state of the form

$$a = a(p, T) \tag{4}$$

where a represents any thermodynamic variable, such as density, enthalpy or speed of sound for instance, expressed in terms of pressure p and temperature T.

2.2 Flow compressibility and equation of state

Typical buoyancy flows occurs at very low speeds, compared to the local speed of sound. Due to a volumetric heat addition, density changes are entirely due to the temperature changes via the compressibility coefficient β, and not to the high fluid speed. It is for this reason that buoyancy flows are mistakenly called "incompressible", with the true meaning of very low Mach number flows. As a result however, the exchange mechanism between internal and kinetic energy, switched on by the gravitational source term of the momentum equation, is the only responsible of fluid motion and the whole system is fully coupled. The most general equation of state for buoyancy flows is $\rho = \rho(p, T)$. A typical model for buoyant flows is to add the body gravitational force as a source term in the momentum equation, as ρg_i, where g_i is the gravity vector component in the i- direction. The hydrostatic pressure gradient can be separated from the the pressure gradient and expressed as $-\rho_0 g_i$, where ρ_0 is evaluated at a reference state; thus the source term simply becomes $(\rho - \rho_0)g_i$. With the Boussinesq approximation the source term is expressed as $-\rho_0 g_i \beta(T - T_0)$.

For gases, the perfect gas equation can be used $\rho = \frac{p}{R_G T}$, and there is not error in the source term for the Boussinesq approximation, being $(\rho - \rho_0)g_i = -\rho_0 g_i \beta(T - T_0)$, with $\beta = \frac{1}{T}$. For liquids, starting from the compressibility coefficients β and χ, a general equation of state can be derived in the form $\rho = \rho(p, T) = \rho_0 \; exp[-\beta \; (T - T_0)] \; exp[-\chi \; (p - p_0)]$. Expanding in Taylor series for small values of the argument $\beta \; (T - T_0)$ and neglecting the pressure dependence the source term becomes $(\rho - \rho_0) g_i \approx -\rho_0 g_i (\beta(T - T_0) - \frac{[\beta(T - T_0)]^2}{2})$. If only the leading term of the expansion is considered, the classical Boussinesq approximation can be recovered. Adding also the second order term a second-order Boussinesq formulation is obtained. With this approach density is kept constant throughout the domain.

2.3 Nondimensional analysis

The application of the Buckingam π theorem to a buoyancy-driven physical system leads to a clear and rigorous nondimensional description. A generic buoyancy-driven system may be characterized by the 6 quantities summarized in table 1. There are 6 quantities with 3 units involved; therefore the number of nondimensional independent parameters of the system is $N = 6 - 3 = 3$. Altought the choice of the parameters is somehow arbitrary, generally the Rayleigh number $Ra = \frac{g\beta\Delta T L^3}{\nu\alpha}$, and the Prandtl number $Pr = \frac{\nu}{\alpha}$ are chosen to describe the system. The third parameter can be for instance $\epsilon = \beta\Delta T$ which can be read as a measure of the compressibility of the system.

Once the choice has been made, all the other nondimensional parameters that can be defined are functions of $Ra, Pr, \beta\Delta T$, for instance, the Nusselt number $Nu = Nu(Ra, Pr, \beta\Delta T)$ and the Reynolds number $Re = Re(Ra, Pr, \beta\Delta T)$.

Quantity	Meaning	units
L	Length	m
α	Thermal diffusivity	m^2/s
ν	Kinematic viscosity	m^2/s
g	Gravity acceleration	m/s^2
β	Thermal expansion coefficient	$1/K$
ΔT	Temperature drop	K

Table 1: Quantities which can be chosen to characterize a buoyancy-driven system.

3 NUMERICAL METHODS

The in-house developed code **Karalis** is used for the calculations. **Karalis** is a parallel MPI, Finite-Volume, multiblock CFD code which solves the fully compressible Euler and Navier-Stokes equations 1,2,3,4 where all couplings between dynamics and thermodynamics are allowed. This is the most general mathematical model for all fluid flows.

The code solves the coupled system of continuity, momentum and full energy equation for the velocity components, pressure and temperature. Once u, v, w, p and T are updated, arbitrary thermodynamics is supplied.

This formulation, typical of aerodynamic flows, shows an ecellent efficiency even for incompressible flows as well as for flows of incompressible fluids (typically buoyancy flows), once equipped with a preconditioner (see [3]).

The most general system of the unsteady Navier-Stokes equations is integrated with an implicit method. The method can stand infinite CFL number and shows the efficiency of a quasi-Newton method independent of the multi-block partitioning on parallel machines.

The whole formulation allows to easily recover the Boussinesq approximation as a special case, setting $\rho = \rho_0$ as equation of state and adding a source term in the momentum equation.

Further details can be found in [4], [5]. For turbulent flows, the turbulence model by Spalart and Allmaras [6] is used for the calculations.

4 RESULTS

4.1 Differentially heated cavity

A differential heated square cavity has been chosen as first test case. The left and right walls are kept at constant temperatures T_{HOT} and T_{COLD} respectively, while the top and bottom walls are adiabatic. The grid used has 64×64 cells and it is stretched to the walls with a maximum to minimum cell ratio of 10. The Rayleigh number has been fixed to $Ra = 10^5$ in the full laminar stationary range, while the Prandtl number is $Pr = 0.71$. The perfect gas law is adopted as equation of state, while the Sutherland law is used to describe the temperature dependence of the diffusion coefficients. Three values of the compressibility parameter have been chosen, namely $\beta\Delta T_{REF} = 0.15, 0.5, 1.2$. The nondimensional temperature is defined as: $T = \dfrac{T - \bar{T}}{\Delta T_{REF}}$ (where $\bar{T} = \dfrac{T_{HOT} + T_{COLD}}{2}$) and varies from $-1/2$ to $1/2$ throughout the domain.

The temperature isolines in the fully compressible cases and with the Boussinesq approximation for different $\beta\Delta T$ are shown in Figure 1. Energy enters in the domain basically from the bottom part of the left hot wall, and leaves through the top part of the right cold wall where isotherms are stretched. Compressibility mainly has a distortion effect of the cold isotherms in the central part of the domain, while the use of the Boussinesq approximation doesn't capture this physical effect. Results are in accordance with those obtained by Chenoweth and Paolucci [2] for the same configuration.

A Nusselt number can be defined on the basis of the wall heat flux as $Nu = \dfrac{q}{q_{COND}}$, where q_{COND} is the pure conductive heat flux. The error made on the Nusselt number by the use of the Boussinesq approximation is represented in Figure 2. Labelling with the pedices $_{FC}$ and $_{B}$ the fully compressible and the Boussinesq cases, an error can be defined as:

$$Err = \frac{Nu_{FC} - Nu_B}{Nu_{FC}} \cdot 100 \tag{5}$$

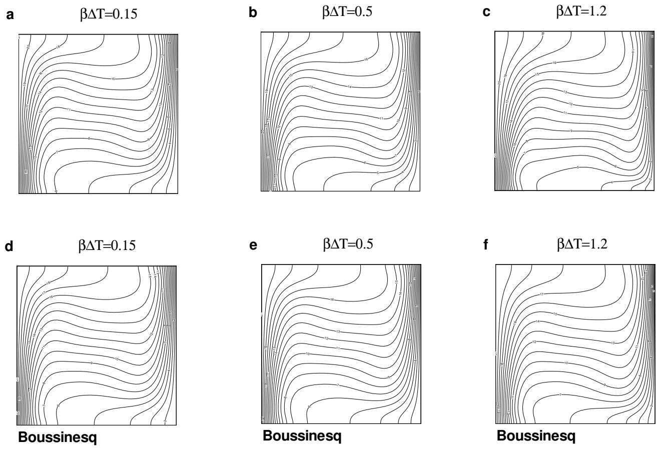

Figure 1: Temperature isolines in the fully compressible case (a,b,c) and with the Boussinesq approximation (d,e,f).

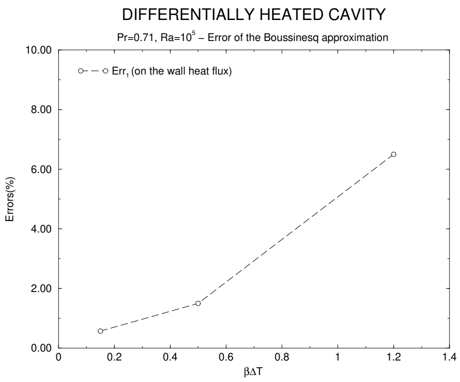

Figure 2: Error of the Boussinesq approximation on the Nusselt number.

The error is less than 7% for $\beta\Delta T = 1.2$.

4.2 Internally heated loop

The two-dimensional motion in an anular loop is driven by buoyancy. A volumetric heat generation is supplied in a sector of the domain at a rate $\dot{Q}$ (per unit volume), and the walls are kept at a constant temperature T_0. The grid used has 60×60 cells and it is stretched to the walls with a maximum to minimum cell ratio of 80. The enclosure is filled with a fluid whose Prandtl number is $Pr = 0.032$, which can represent for instance a liquid metal. The internal and the external radius measures L and $2L$ respectively. A reference temperature drop is defined on the basis of pure conduction in an infinite slab of width L

$$\Delta T_{REF} = \frac{\dot{Q}L^2}{8\lambda} \tag{6}$$

The Rayleigh number is computed on this basis and it has been fixed to $Ra = 500$ for all the simulations within the laminar stationary range. The Nusselt number has been defined as a nondimensional temperature drop:

$$Nu = \frac{\Delta T_{MAX}}{\Delta T_{REF}} \tag{7}$$

A Reynolds number can be defined on the mass flow rate $\dot{m}$, the molecular viscosity μ and the duct cross-section A:

$$Re = \frac{\dot{m}L}{\mu A} \tag{8}$$

and it is a measure of the intensity of motion originated by the buoyant force. Velocity is made dimensionless through a refence free fall velocity in the modified buoyancy gravity field:

$$v_{REF} = \sqrt{g\beta\Delta T L} \tag{9}$$

Four values of the compressibility coefficient $\beta\Delta T$ have been considered, i.e. $\beta\Delta T = 0.1, 0.3, 0.6, 0.9$.

Due to the internal heat generation temperature rises up in the heated sector, and the fluid moves clockwise. The velocity and temperature isolines in the fully compressible case for $\beta\Delta T = 0.1$ are shown in Figure 3 and 4 respectively as examples of typical fields. In Figure 5 velocity profiles at the duct centerline are shown in the fully compressible cases as functions of the azimuthal angle Ψ ($\Psi = 0$ represents the inlet of the heated sector). The effect of compressibility is small for $\epsilon = 0.1$, while it leads to a completely different situation for higher $\beta\Delta T$, with an evident velocity peak due to the lower local density and the the stonger coupling. Figure 6 shows the same quantity in the fully compressible and the Boussinseq (1^{st} and 2^{nd} order) cases for $\beta\Delta T = 0.6$. Altough the error on the mass flow rate, tied to the ground level of the curves, is reduced with the 2^{nd} order approximation as a consequence of the reduced error on the buoyant source term, the high peak of the fully compressible curve is not reproduced. Therefore this effect is entirely due to the coupling between the equation of state and the continuity equation and leads to a qualitatively different flow structure. For $\beta\Delta T = 0.9$, the fully compressible calculation exhibits a boundary layer separation, well evidenced by the streamlines in Figure 7. This effect can be understood by considering the pressure distribution in Figure 8; there is basically a radial gradient which balances the centrifugal force, but in the separation zone there is also an adverse pressure gradient in the flow direction.

The error of the Boussinesq approximation on the main dependent parameters can be defined in a similar way as in subsection 4.1. The error on the Nusselt number is shown in Figure 9. The behaviour is linear with $\beta\Delta T$ and values are limited to a few percent. The Error on the Reynolds number is much more consistent, see Figure 10. The error exhibits a linear behaviour for $\beta\Delta T < 0.6$; the last point is strongly influenced by the separation region. As already pointed out, such an error is substantially reduced by the use of a 2^{nd} order Boussinesq approximation (see Figure 6).

4.3 Internally heated-cooled loop

A similar geometric configuration to that of subsection 4.2 is presented here. Heat is volumetrically supplied in a sector of

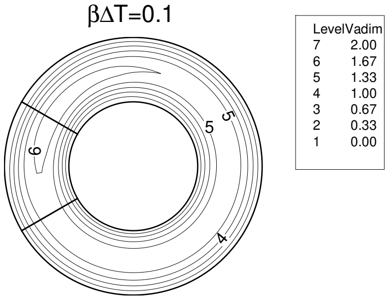

Figure 3: Velocity isolines in the fully compressible case for $\beta\Delta T = 0.1$.

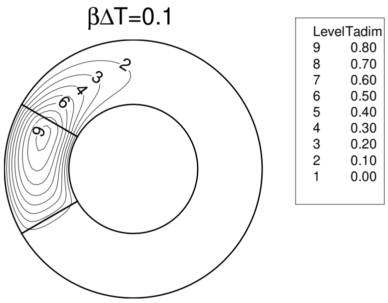

Figure 4: Temperature isolines in the fully compressible case for $\beta\Delta T = 0.1$

the domain (on the left) as in the previous case, but it is symmetrically subtracted in another sector of the domain. At the walls the adiabatic conditions are imposed. The grid used for the calculations is the same as in the previous case (subsection 4.2). The enclosure is filled with a fluid whose Prandtl number is $Pr = 1.18$, which can represents for instance water at $400K$. The internal and the external radius measures L and $2L$ respectively. A reference velocity v_{REF} can be expressed as in the previous case (equation 9), while a reference temperature drop can be here fixed on the basis of the global energy balance:

$$2\dot{Q}\Omega_H = \rho v_{REF} A c_p \Delta T \tag{10}$$

where Ω_H is the heated volume, and A is the cross section of the anulus. The resulting reference temperature drop can be expressed as:

$$\Delta T_{REF} = \left(\frac{\pi^2 \dot{Q}^2 L}{\rho^2 c_p^2 g\beta} \right)^{\frac{1}{3}} \tag{11}$$

The Rayleigh number computed using this reference temperature drop varies from 1.6×10^9 to 7.3×10^9 in the fully turbulent range. In this context, it is not really important that Ra is strictly constant for the different cases because the interest is focussed on the effects of compressibility on the solution. A nondimensional temperature can be defined as:

$$T = \frac{T - \bar{T}}{\Delta T_{REF}} \tag{12}$$

where $\bar{T}$ is an average temperature based on energetic concepts:

$$\bar{T} = \frac{\int_\Omega \rho c T d\Omega}{\int_\Omega \rho c d\Omega} \tag{13}$$

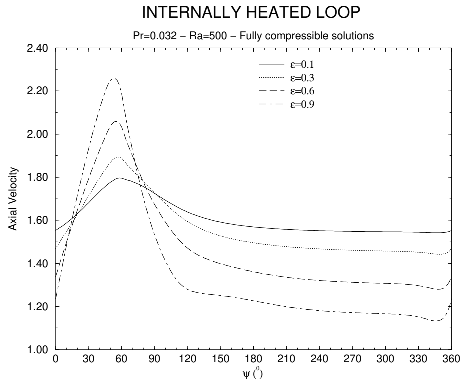

Figure 5: Velocity profiles at the duct centerline in the fully compressible cases. $\Psi = 0$ is located at the inlet of the heated sector.

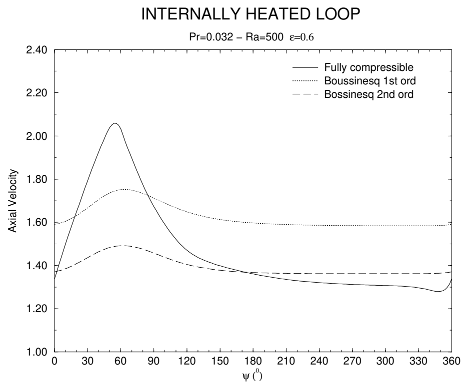

Figure 6: Velocity profiles at the duct centerline for $\beta\Delta T = 0.6$. Fully compressible, Boussinesq 1^{st} and 2^{nd} order solutions are compared.

where the integral is computed over the whole fluid domain Ω and c is the specific heat. The nondimensional velocity and temperature isolines in the fully compressible case for $\beta\Delta T = 0.15$ are shown in Figure 11 and 12 respectively. The fluid moves clockwise and it is heated and cooled in the sectors on the left and on the right respectively. At a first approximation, neglecting the effects of energy diffusion, heat is basically added (or subtracted) along each streamline at a constant rate. Therefore the temperature at the outlet of the heated (sinked) block depends on the crossing time; as a consequence, the maximum (minimum) temperature will be localized in the velocity boundary layer at the end of the active sectors. Diffusion only justifies the spreading of the isolines close to the inter-block boundaries.

The nondimensional velocity profiles at the duct centerline are shown in Figure 13 as functions of the azimuthal angle Ψ. The two peaks correspond to the active blocks, while different levels of velocity along the centerline are tied to the different densities ($\Psi > 240$ cold region, high density).

The error of the Boussinesq approximation on the evaluation of the Reynolds number is shown in Figure 14. The error scales linearly with the compressibility parameter and is about 9% for the highest $\beta\Delta T = 0.43$.

5 CONCLUSIONS

An assessment of the Boussinesq approximation has been performed by the use of numerical simulations. Boussinesq results

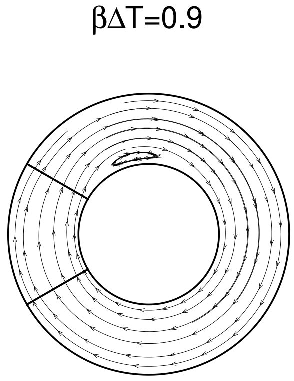

Figure 7: streamlines in the fully compressible case for $\beta\Delta T = 0.9$.

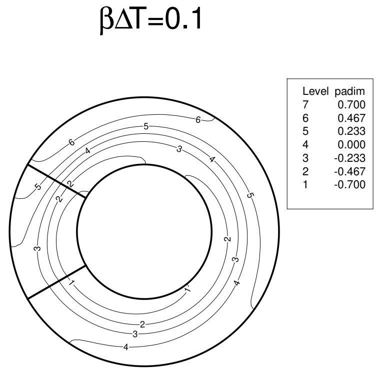

Figure 8: Pressure isolines in a fully compressible case ($\beta\Delta T = 0.1$).

have been compared with fully compressible 'exact' solutions for different values of a compressibility parameter $\beta\Delta T$. There are two source of errors in the Boussinesq approach, one tied to the source term in the momentum equation and the other one tied to the coupling between the equation of state and the continuity equation. For gases, due to the special form of the state equation, the first source of errors is absent and the error on the performance parameters is limited to a few percent. For liquids, the error on the performance parameters can reach 20% or more. At a deeper investigation, using a second order Boussinesq expression of the buoyant source term, the global error is reduced drastically to a few percent. Nevertheless, there are some special features of the flow field tied only to the compressible coupling between the state and the continuity equation. These details of the physics of motion can only be captured in a compressible framework.

6 REFERENCES

1. H. Paillere F., C. VIozat, A. Kumbaro, I. Toumi, Comparison of low Mach number models for natural convection problems, *Heat and Mass Transfer*, vol. 36, pp. 567-573, 2000.

2. D.R. Chenoweth and S. Paolucci, Natural convection in an enclosed vertical air layer with large horizontal temperature diffrences, *J. Fluid Mechanics*, vol. 169, pp. 173-210, 1986.

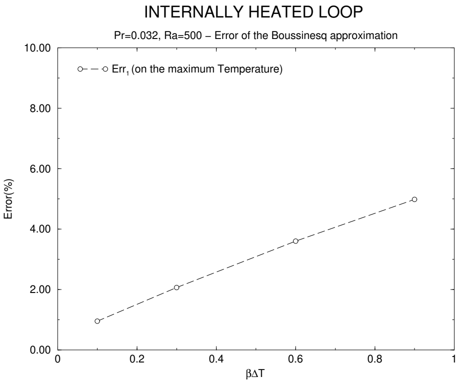

Figure 9: Error of the Boussinesq approximation on the Nusselt number.

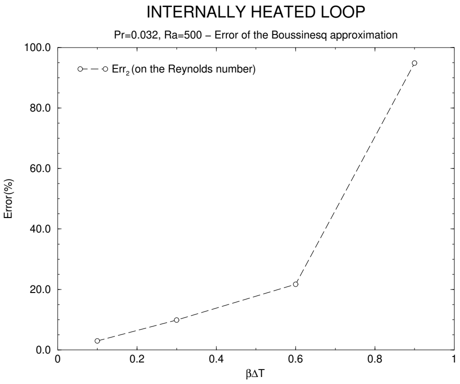

Figure 10: Error of the Boussinesq approximation on the Reynolds number.

3. C.L. Merkle, J.Y. Sullivan, P.E.O. Buelow and S. Venkateswaran, Computation of flows with arbitrary equation of state, *AIAA Journal*, vol.36, no.4, 1998.

4. M. Mulas, S. Chibbaro, G. Delussu, I. Di Piazza and M. Talice, The CFD Code Karalis, CRS4-TECH-REP 00/87, 2000.

5. M. Mulas, S. Chibbaro, G. Delussu, I. Di Piazza and M. Talice, Efficient parallel computations of flows of arbitrary fluids for all regimes of Reynolds, Mach and Grashof numbers, to be published in *International Journal of Numerical Methods for Heat & Fluid Flow*, special issue edited by G.Comini, 2002.

6. P.R. Spalart and S.R. Allmaras, A one-equation turbulence model for aerodynamics flows, *La Recherche Aerospatiale*, no. 1, 1994.

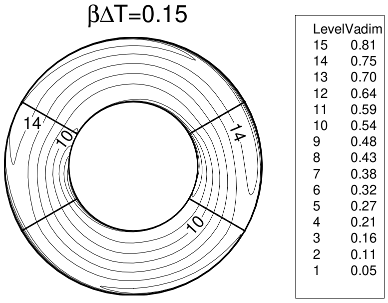

Figure 11: Velocity isolines in the fully compressible case for $\beta\Delta T = 0.15$.

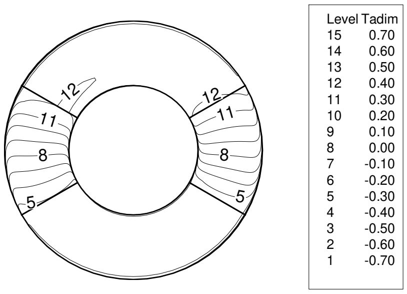

Figure 12: Temperature isolines in the fully compressible case for $\beta\Delta T = 0.15$.

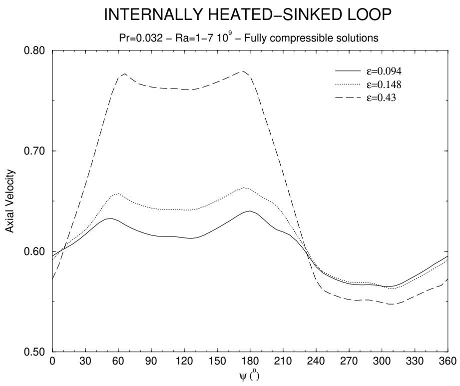

Figure 13: Velocity profiles at the duct centerline in the fully compressible cases. $\Psi = 0$ is located at the inlet of the heated sector.

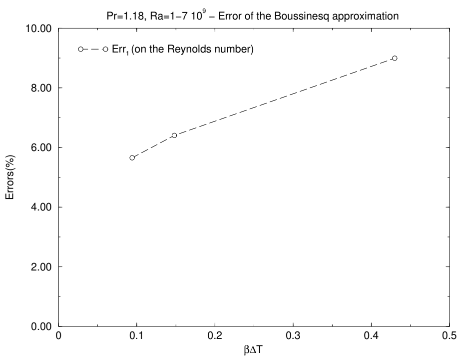

Figure 14: Error of the Boussinesq approximation on the Reynolds number.